

Estimation of cavitation intensity from the time taken for bubbles to develop

H. Soyama^{a,*} and M. Futakawa^b

^aDepartment of Mechanical Engineering, Tohoku University, Aoba 6-6-01, Aramaki, Aoba-ku, Sendai, 980-8579, Japan

^bJapan Atomic Energy Agency, Tokai-mura, Naka-gun, Ibaraki-ken, 319-1195, Japan

Received 22 June 2006; accepted 19 July 2006; published online 12 August 2006

In order to estimate the cavitation erosion rate, the time taken for cavitation bubbles to develop and the cavitation erosion intensity were investigated. The cavitation intensity was found to be proportional to the 7th power of the time taken for bubbles to develop. This is a similar dependency to the effect of scaling on cavitation erosion, which shows how the cavitation erosion rate increases with cavitating length.

KEY WORDS: cavitation erosion, hydraulic systems, intensity, cavitating length

1. Introduction

In a joint project between the Japan Atomic Energy Agency (JAEA) and the High Energy Accelerator Research Organization (KEK), a MW-scale spallation neutron source is being constructed for use in research in new areas of science such as materials and the life sciences. The neutron source is being constructed at the Japan Proton Accelerator Research Complex (J-PARC) [1]. Liquid mercury will be used as both the target and coolant. However, Kass *et al.* [1] revealed that cavitation erosion rate for stainless steel in mercury increased in a nonlinear fashion with applied power using a vibratory erosion test. Futakawa *et al.* [2–8] found that severe cavitation erosion can occur in the wall of the target vessel. As the thickness of the wall of the vessel is 2.5 mm, it is essential to establish a method for estimating the lifetime of the vessel, and several methods have been proposed [9–11].

In the target vessel in J-PARC, cavitation is generated by a pulsed proton beam with a pulse duration and pulse rate of 1 μ s and 25 Hz, respectively [2]. When the proton beam hits the mercury in the target vessel, a thermal shock is generated and the impact pressure waves from the thermal shock propagate to the wall of the target vessel causing the vessel to vibrate, which in turn gives rise to cavitation in the mercury close to the vessel wall. This cavitation produces pitting in the wall of the target vessel. Pitting caused by injecting a pulsed proton beam into mercury has been confirmed [6,7]. The

cavitation intensity in the target vessel depends on the power of the proton beam in the spallation neutron source. In order to predict the erosion rate, the cavitation intensity needs to be estimated. Although the cavitation intensity seems to be related to the amplitude of the high frequency components of the vibration excited by proton bombardment, measurement of the amplitude is difficult and not very accurate, since the target vessel is set in a safety hull and the path by which the vibration travels is complex. The time for cavitation bubbles to develop at each cycle is one of parameters associated with the cavitation intensity, as larger cavitation bubbles are likely to produce a larger impact. On the other hand, the time for cavitation bubbles to develop is related to the size of the hydraulic machinery, i.e., there is a scaling effect in cavitation erosion. Cavitation erosion becomes drastically more aggressive as the size of machine increases. When the size of the hydraulic machinery gets larger, the cavitating length gets longer, and consequently the time for bubbles to develop is longer at constant flow velocity. It is crucial to measure a parameter, such as the time for bubbles to develop, in order to investigate the scaling effect of cavitation erosion.

In the present paper, in order to predict the cavitation erosion rate of target vessels and to study the scaling effect of cavitation erosion, the time for cavitation bubbles to develop and the cavitation erosion rate were examined using a Magnet IMPact Testing Machine (MIMTM) [9]. The dependencies of rate of erosion on the development time for bubbles in MIMTM and the cavitating length in hydraulic machinery were shown to be similar.

*To whom correspondence should be addressed.
E-mail: soyama@mm.mech.tohoku.ac.jp

2. Experimental facilities and procedures

Figure 1 shows a schematic diagram of the mercury chamber in MIMTM. The plate specimen, which is electrically driven by the pressure pulse actuator, is connected to a short cylinder filled with mercury, whose capacity is about 120 cc. In order to change the cavitating conditions, the driving impact force of the plate specimen can be changed by altering the voltage applied to the pressure pulse actuator.

In order to measure the time for cavitation bubbles to develop, a laser Doppler vibrometer was used to detect the vibration corresponding to bubble collapse, as high frequency vibration is produced as the bubble collapses. The acceleration of the plate specimen was also measured. Figure 2 shows a schematic diagram of the measurement system. A 5 kHz high-pass filter and a 100 kHz low-pass filter were used as a band-pass filter for the signal from the laser Doppler vibrometer. The sensitivity of the laser Doppler vibrometer was 0.05 (m/s)/V.

In order to measure the cavitation erosion intensity in MIMTM, the surface of the plate specimen was examined for erosion to assess the coverage on the surface in the early stages of the incubation period. The coverage C is defined as the fraction of the area damaged on the surface. The cavitation erosion intensity is obtained as follows [11]:

1. Measure the coverage in the early stages of incubation.
2. Obtain the constant a in Eq. (1).

$$C = 1 - e^{at} \quad (1)$$

3. Obtain the incubation time from the Eq. (1) at $C = 0.98$, i.e., 98%. The cavitation intensity is the inverse of the incubation time [11].

In order to investigate the correlation between the scaling effect and the time for cavitation bubbles to develop, the result of scaling on hydrofoils was also examined. The scaling effect of the hydrofoils was investigated by measuring the variations in the acoustic power and the plastic deformation pits when the chord length was varied from 53 to 160 mm at constant flow velocity [12,13]. The hydrofoil was set in the cavitation

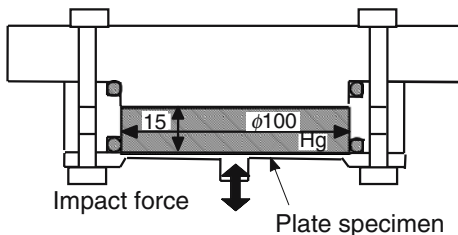


Figure 1. Mercury chamber in MIMTM.

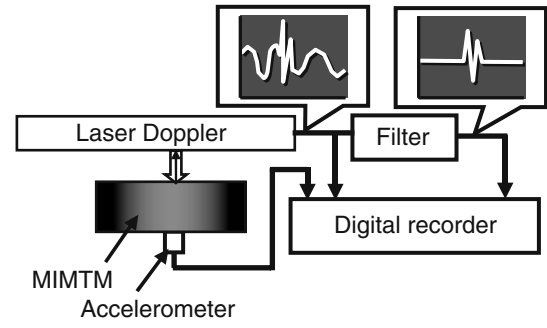


Figure 2. Schematic diagram of measuring system.

tunnel and the acoustic power was measured by hydrophone. Plastic deformation pits on a thin aluminum plate placed on the hydrofoil were measured. The cavitation intensity was calculated from the acoustic noise and the plastic deformation pits.

3. Results

Figure 3 shows the output signal of the acceleration, the vibration without the band-pass filter and the vibration with the band-pass filter as a function of time t using MIMTM. When the plate specimen was driven by the magnetic force, cavitation was produced in the mercury and the bubbles collapsed at $t \approx 2$ ms, as the high frequency components related to cavitation bubble collapse are superimposed on the measured vibration at around 2 ms after actuating the plate. Using the band-pass filter, the high frequency components become much clearer. The time from when the plate is first driven to the maximum amplitude is related to the time for bubbles to develop. In the present paper, the development time t_d is defined as the time between actuating the plate and that at which the bubble collapses, which occurs when the maximum amplitude of the high frequency signal is detected, as shown in figure 3.

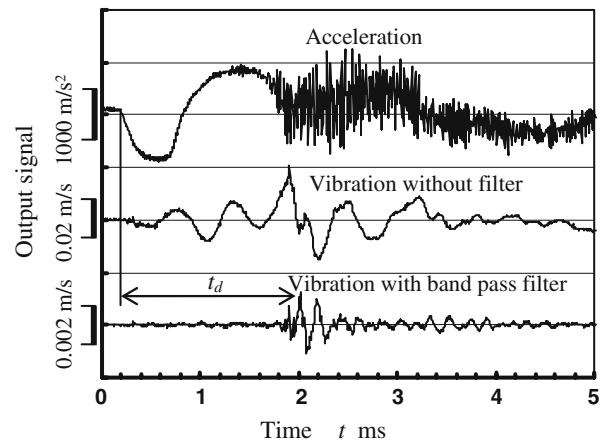


Figure 3. Output signal of accelerometer and laser Doppler vibrometer.

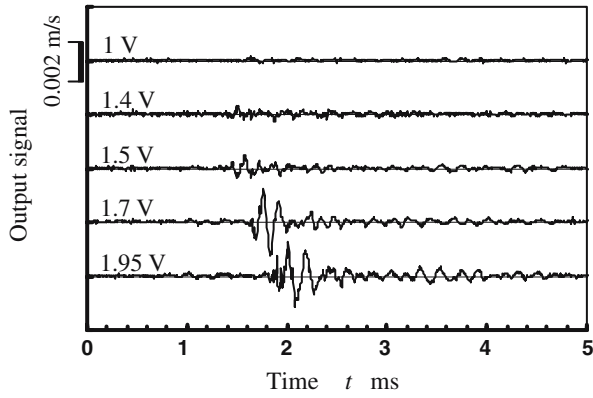


Figure 4. Variation of the vibration measured using a laser Doppler vibrometer with cavitating conditions.

Figure 4 shows the output signal from the laser Doppler vibrometer through the band-pass filter under different cavitation conditions, i.e., different voltages applied to the pressure pulse actuator. The amplitude of the vibration and the time t_d increase with increasing voltage from 1.4 to 1.95 V. At an applied voltage of 1 V, cavitation erosion was scarcely observed. The results show that cavitation bubbles develop further and the cavitation erosion intensity increases with voltage.

Table 1 shows the time t_d and the coverage of the cavitation damage on the eroded surface. The coverage was measured after 10^5 cycles. In the present paper, the erosion time is the number of cycles of the applied driving force. Thus, the incubation time refers to the number of cycles in the incubation period. From Eq (1), the number of cycles in the incubation period n_i was obtained from the coverage for each condition. The inverse value of n_i is proportional to the cavitation intensity. The normalized cavitation intensity was calculated from n_i normalized to its value at $V_p = 1.4$ V. The time t_d was measured 10 times and averaged for each condition.

Figure 5 reveals the relationship between the estimated time for cavitation bubbles to develop t_d and the cavitation intensity I_{cav} . The development time and the cavitation intensity are normalized by their values at $V_p = 1.4$ V. The results of the scaling effect on hydrofoils are also plotted in figure 5, in order to illustrate the correlation between the scaling effect and the development time for cavitation bubbles. In the case of the

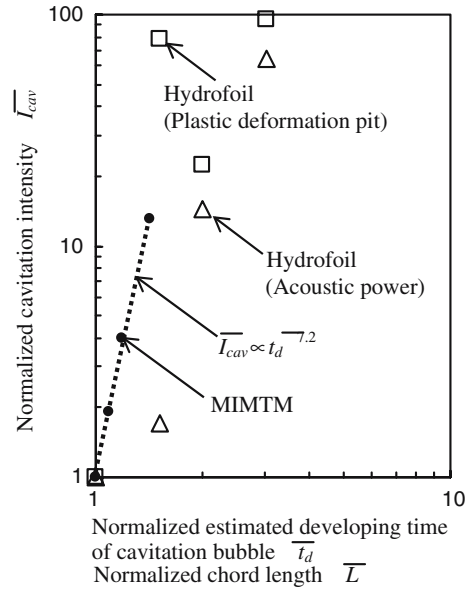


Figure 5. Plots showing the similar dependency of cavitation erosion on the time for cavitation bubbles to develop and on scaling.

hydrofoil, the chord length L and the cavitation intensity are normalized by their values at $L = 53$ mm. The cavitation intensity increases with development time, and applying a power law shows the exponent n to be 7.2. That is, the cavitation erosion intensity increases approximately as the 7th power of the development time. The cavitation intensity using the hydrofoil also increases dramatically with chord length. Even though the results are scattered, the dependency of I_{cav} on t_d for the hydrofoil measurements is similar to that of the results from the experiments using MIMTM.

Figure 6 illustrates the relationship between the input power P_{in} and the estimated time for cavitation bubbles to develop t_d . This shows that t_d increases with the square root of P_{in} . Since the results above show that the I_{cav} increases with t_d to the power of 7.2, it increases with input power P_{in} to the power of 3.6. Pressure pulse tests done at the Weapon Neutron Research WNR of the Los Alamos Neutron Science Center LANCE and MIMTM of JAEA have shown the cavitation erosion intensity to increase with a 3.8 power law dependency on input power [10]. This agrees well with the result obtained here. Thus, monitoring the high frequency

Table 1. Input power of pressure pulse actuator, time for cavitation bubbles to develop and cavitation intensity.

| Voltage applied to pressure pulse actuator V_p V | Input power P_{in} W | Estimated time for cavitation bubbles to develop t_d ms | Coverage C | Number of cycles of incubation period n_i | Normalized cavitation intensity I_{cav} |
|--|------------------------|---|--------------|---|---|
| 1.4 | 294.2 | 1.84 ± 0.51 | 0.101 | 3.69×10^6 | 1.0 |
| 1.5 | 340.6 | 1.73 ± 0.15 | 0.184 | 1.93×10^6 | 1.9 |
| 1.7 | 438.0 | 2.11 ± 0.05 | 0.346 | 9.27×10^5 | 4.0 |
| 1.95 | 556.5 | 2.76 ± 0.17 | 0.752 | 2.82×10^5 | 13.1 |

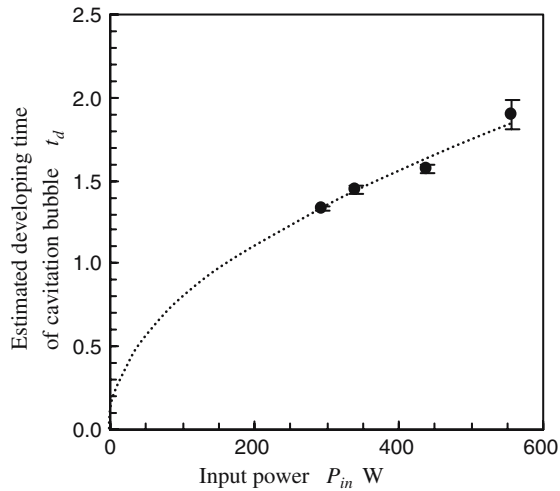


Figure 6. Relationship between the input power and time for cavitation bubbles to develop.

components of the vibration, which is related to bubbles collapsing, is a good method for predicting cavitation intensity. This can be used to estimate the cavitation intensity of the target vessel used for the spallation neutron source.

4. Conclusions

In order to estimate the cavitation erosion intensity in the target vessel of a spallation neutron source, the time for cavitation bubbles to develop was examined as a function of cavitation erosion. It can be concluded that the time for the bubbles to develop can be used in estimating the cavitation erosion intensity.

References

- [1] M.D. Kass et al., Tribol. Lett. 5-2-3 (1998) 231.
- [2] Planning Div. Neutron Sci., Proc. 3rd Workshop Neutron Sci. Project, 1999.
- [3] M. Futakawa et al., J. Phys. IV France 10 (2000) 237.
- [4] M. Futakawa et al., Nucl. Instrum. Methods Phys. Res. 439 (2000) 1.
- [5] M. Futakawa et al., Inter. J. Impact Eng. 28-2 (2003) 123.
- [6] B. Riemer, Proc. 3rd Inter. WS Mercury Target Development ORNL, 2001.
- [7] J.R. Haines et al., SNS-101060100-TR0004-R00, 2002.
- [8] S. Ishikura et al., J. Nuclear Mater. 318 (2003) 113.
- [9] H. Soyama and M. Futakawa, Tribol. Lett. 17-1 (2004) 27.
- [10] M. Futakawa et al., J. Nuclear Mater. 343 (2005) 70.
- [11] H. Soyama et al., J. Nuclear Mater. 343 (2005) 116.
- [12] H. Soyama et al., Proc. Inter. Symp. Cav. Noise Erosion Fluid Sys., FED- 88 (1989) 41.
- [13] H. Soyama, Trans. JSME 58 (1992) 3366.